2011 IEEE/RSJ International Conference on
Intelligent Robots and Systems
September 25-30, 2011. San Francisco, CA, USA

Active Target Localization for Bearing Based Robotic Telemetry

Pratap Tokekar, Joshua Vander Hook and Volkan Isler

Abstract— **We present a novel robotic telemetry system for localizing radio-tagged invasive fish in frozen lakes using coarse bearing measurements. We address the problem of selecting sensing locations so as to minimize the uncertainty in the location of the target. For this purpose, we propose three active localization algorithms and evaluate them both in simulations and through field experiments. We also present a novel technique for bearing-estimation from directional radio antenna which is critical for the successful execution of the active localization algorithms. Our system is able to operate on frozen lakes and localize the target to within values as low as one meter.**

I. Introduction

Telemetry technology allows measuring information about a target from a distance. It has a wide range of applications ranging from defense to fisheries and wildlife research. For example, researchers at the University of Minnesota tag invasive fish with radio transmitters and track their movement in lakes [1]. Similar systems exist for tracking various fish, reptiles and birds [2]–[4].

In this paper, we present a tracking algorithm along with field results for a novel robotic telemetry system. The domain application for our system is tracking Common Carp in Minnesota's lakes. Carp is a highly invasive fish which pollutes lakes and destroys the natural habitat of the native animals. In an effort to control carp, agencies and municipalities often resort to non-selective toxins (in other words, poison) which themselves are ecologically damaging. Recent research of the Sorensen Lab at the University of Minnesota revealed that carp strongly aggregate in winter. If these aggregations can be detected, carp can be netted. This provides an ecologically friendly solution to the carp problem.

Unfortunately, carp aggregations are unpredictable. As a result, researchers spend a long time on frozen lakes trying to localize fish manually. Our goal is to replace this manual effort with robots. Toward this goal, we developed a field robot capable of localizing tagged fish (see Figure 1). The underlying telemetry technology used by the fisheries researchers introduces a challenging active localization problem: each tag emits a signal at a dedicated frequency once every second. A directional antenna can be rotated to find the bearing of the fish but as shown in Section III the uncertainty in these measurements is rather large. We use multiple measurements taken at various locations to estimate the location of the target. The problem we address in this paper is how to choose sensing locations in an online fashion so as to accurately localize a stationary fish with a small number of measurements.

This work is supported by NSF Awards #0916209, #0917676, #0936710, #0934327 and a fellowship from the Institute on the Environment at the University of Minnesota. The authors are with the Department of Computer Science and Engineering, University of Minnesota, Minneapolis, MN, USA. {tokekar,jvander,isler}@cs.umn.edu

Fig. 1. The A100 Husky with tracking equipment (left top of chassis) and antenna during field testing on Lake Casey, MN.

Our results and organization of the paper: In Section III, we present an overview of our system and describe the algorithms for bearing estimation. Next in Section IV, we show how the robot can obtain a good initial estimate of the target location. We then investigate three algorithms for choosing the sensing locations. The first one is an open-loop strategy based on the Cramer-Rao Lower Bound. The next two are online algorithms which incorporate measurements as they become available. We compare the algorithms in simulations and through real experiments in Section V. The experiments show that we can localize the target to within approximately one meter. We start with an overview of related work.

II. Related Work

The literature on bearing-only localization and tracking using a robot can be divided into two main areas: improving the estimation performance by designing efficient estimators, and optimizing the trajectory of the robots to obtain more informative measurements. In this paper, we focus only on optimizing the motion of the robot to improve the localization performance.

In one of the earlier works on this problem, Hammel et al. [5] used the determinant of the Fisher Information Matrix (FIM) as the objective function, and numerically computed the optimal trajectory for the robot in the case of continuous measurements. Oshman and Davidson [6] later generalized this problem by adding state constraints on the position of

978-1-61284-456-5/11/$26.00 ©2011 IEEE

the robot and used numerical optimal control techniques to derive the robot trajectory. Bishop and Pathirana [7] derived the optimal motion using FIM with additional final position constraints. The resulting trajectory is computed numerically, and follows a similar spiral pattern as that in [5].

Logothetis et al. [8] used the mutual information between measurements and target trajectory to derive optimal robot trajectory using enumeration and dynamic programming. Computing the mutual information and FIM requires knowing the true location of the target. In practice, we have only an initial estimate of the target. Additionally, all the above described methods present open-loop trajectories for the robot, which do not depend on the actual measurements we obtain. Frew [9] presented a closed-loop strategy for tracking targets using bearing information obtained from monocular vision. The strategy is based on a state-exploration tree, and a trajectory is obtained using breadth-first search for minimum uncertainty. Skoglar et al. [10] pose a similar problem using Information filters and find sub-optimal trajectories using stochastic optimal control for minimizing the determinant of the posterior Information.

One aspect that differentiates our work from the previous work is that our measurements are time consuming. Hence, we can only afford a few measurements. We build on the previous work and evaluate three algorithms for our application and report field results.

III. System Description

The overall system is composed of a ground robot, with the necessary radio equipment mounted on top of it (Figure 1).

A. Robot

Our system is built on a commercial platform: the Husky A100 from Clearpath Robotics. It is a six-wheeled differential drive chassis with 150 mm tires. Two lead-acid batteries provide approximately three hours of operation time, with a top speed of 1.5 meters per second. High-level processing such as tracking and navigation is handled by an ASUS Eee PC mounted inside the electronics enclosure on Husky. A Garmin 18x GPS unit is used for autonomous waypoint navigation. We approximate the six-wheel differential drive using a unicycle model. State (position and orientation) estimates for the robot are obtained through an Extended Kalman Filter (EKF) fusing GPS and odometer readings. All software was written using ROS from Willow Garage to interface the various components.

B. Radio Antenna

For sensing the fish, we use radio tags provided by Advanced Telemetry Systems (ATS). A complete fish sensing system by ATS consists of radio tags, a loop antenna connected to a radio receiver and a datalogger which provides computer interface for the receiver. Each radio tag emits a pulse of unique frequency, roughly once per second.

The receiver can be programmed to tune on a particular frequency and needs to stay tuned for a duration slightly longer than that. While the signal strength of the received signal depends on the distance of the tag from the antenna, it is not directly useful as it depends on a number of environmental factors such as depth of the fish, salinity and temperature of the water and remaining battery on the tag. Therefore, we rely only on the directional nature of the antenna and obtain a bearing measurement towards the fish. Our method for estimating the bearing is presented next.

C. Measurement model

The strength of the received signal varies with the relative angle of the plane of the loop antenna with the tag. If the tag is directly aligned with this plane, the signal strength is highest. Over 360° of measurements, a noiseless signal is a bimodal function, reaching a maxima at the true bearing, and a second maxima offset by 180°. Minima are measured perpendicular to the target bearing. We mount the antenna on a pan-tilt unit, so that we can rotate it and sample signal strength as a function of the relative angle from the boat.

Figure 2 shows a subset of the samples obtained by rotating the antenna in steps of 15° over $[-90^\circ, 90^\circ]$. The true bearing angle is -30°. As we can see, the values around the true bearing are all high. This makes finding a single bearing direction from the maximum signal value difficult. Instead, we fit a function to the samples obtained, and find the maximum value of this function. We tried both a sinusoidal and a cubic function with least-squares and RANSAC as fitting methods. Both functions agree with the expected behavior of the signal strength as a function of the angle. The data logger reports zero signal-strength if the received strength is under a factory-set threshold. In cases where only a few non-zero values are present in a 180° sweep, fitting a sine using either method or a cubic using RANSAC method do not perform well. Based on a number of trials, we concluded that least squares fitting of a cubic polynomial works best for computing the bearing angle as it gave the best performance. We found this reliably estimated the bearing to the tag to within 15°.

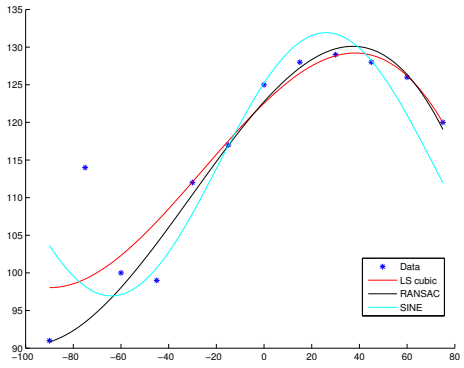

Fig. 2. A coarse sampling and the corresponding estimates. The horizontal axis is the bearing and the vertical is the measured signal strength. In general, least squares estimation of a cubic polynomial provided the best estimates.

To update the estimate of the target, we augment the state of the robot with the position of the tag. We assume the fish

remain stationary during the localization process, hence the EKF propagation does not change the state of the fish. The bearing measurements obtained using the method described above are used to update the joint state of the robot and the tag. The posterior covariance after EKF updates represents the uncertainty in localization, and depends on the sensing location. Since measuring the bearing takes time (around one minute per measurement), estimation of the tag location must be performed using a small number of measurements. In the next section, we present a strategy to carefully choose these sensing locations to minimize the uncertainty.

IV. Active Localization

We present three strategies to compute k sensing locations and compare their performance in simulations and real-experiments. These locations must be chosen in an online fashion as the data becomes available since the location of the fish is not known in advance. All three active localization strategies we present require an initial estimate of the target. Therefore, we address the problem of obtaining an initial estimate first.

A. Initialization

We use two measurements from different sensing locations to initialize the uncertainty of the robot. We draw cones about each bearing obtained: width of the cone represents the sampling interval and noise in measurements. We fit an ellipse about the intersection of the two cones, and initialize the covariance matrix of the target using sigma values obtained from this ellipse.

Uncertainty in the target's location, after the initialization step depends on the relative position of the two sensing locations and the true target location. The first measurement is taken from the starting location $(0, 0)$. Without loss of generality assume that the first bearing measured is aligned with the X-axis. Since the radio tags have a minimum and maximum range (r_{min}&r_{max}), the target can lie anywhere on the X-axis within this range, say at $(r, 0)$. The uncertainty measure for two bearing locations is given by the inverse of determinant of the corresponding Fisher Information Matrix [6] as:

$$U = \left| \frac{d_1 d_2}{\sin\theta} \right|, \tag{1}$$

where d_1 and d_2 are the distances of the two measurement location from the target, and θ is the relative angle between them. Since true target location is unknown and can lie anywhere between $(r_{min}, 0)$ and $(r_{max}, 0)$, the following lemma shows how to choose the second sensing location such that the uncertainty in the worst-case is minimized.

Lemma 1: If the second measurement is taken from $(\frac{r_{max}+r_{min}}{2}, \pm\frac{r_{max}-r_{min}}{2})$, the worst-case uncertainty in the target's position after two measurements is minimized.

Proof: Assume the robot moves to (x, y) to take the second measurement. If the target is located at $(r, 0)$, our resulting uncertainty is given by,

$$U = \left| \frac{r\sqrt{(x-r)^2+y^2}}{\sin\theta} \right| = \left| \frac{r\sqrt{(x-r)^2+y^2}}{\frac{y}{\sqrt{(x-r)^2+y^2}}} \right|,$$
$$= \left| \frac{r((x-r)^2+y^2)}{y} \right|.$$

Our objective here is to pick (x, y) to minimize U over all possible values of $r \in [r_{min}, r_{max}]$. By differentiating U with respect to y, we find that for a given r and x, the minima occurs at $y = \pm(x - r)$. Intuitively, we see that x must be at $\frac{r_{min}+r_{max}}{2}$. Otherwise, it is closer to either r_{max} or r_{min} and by selecting r to be r_{min} and r_{max} respectively, we can increase U. We can formally prove this by letting $x = \beta\frac{r_{max}+r_{min}}{2}$ and showing that for both $\beta < 1$ and $\beta > 1$, the maximum value of U we obtain is higher than that for $\beta = 1$. Hence, the optimal choice for the second measurement is $x = \frac{r_{max}+r_{min}}{2}$ and $y = \pm\frac{r_max-r_{min}}{2}$. ■

With this initial estimate obtained, we now use the following three strategies to determine the k sensing locations for the robot. The actual estimate of the target after obtaining each measurement is computed using the EKF.

B. Cramer-Rao Lower Bound

The Cramer-Rao lower bound for an unbiased estimator $\hat{X}$ of state X is a lower bound on the estimation error covariance matrix P_k given as,

$$P = E[(X - \hat{X})^T(X - \hat{X})] \geq I^{-1},$$

where I is the FIM for the k measurements. For k bearing measurements with zero-mean Gaussian noise, I can be expressed as [6],

$$\mathbf{I} = \sum_{i=1}^{k} \frac{1}{\sigma^2 d_i^4} \begin{bmatrix} \Delta y_i^2 & -\Delta x_i \Delta y_i \\ -\Delta x_i \Delta y_i & \Delta x_i^2 \end{bmatrix}$$

where $\Delta x_i = (x_r(i) - x_t)$, $\Delta y_i = (y_r(i) - y_t)$, and $d_i^2 = \Delta x_i^2 + \Delta y_i^2$. Here, $(x_r(i), y_r(i))$ is the location of the robot for the i^{th} measurement, and (x_t, y_t) is the true target location.

The determinant of the FIM defined above is inversely proportional to the square of the area of the 1-σ uncertainty ellipse. Hence, the determinant of I is commonly used as the objective function to maximize. The determinant of I can be expressed as,

$$|I| = \frac{1}{\sigma^4} \sum_{i=1}^{k} \sum_{j=1}^{k} \left[\frac{\sin(\theta_i - \theta_j)}{d_i d_j} \right]^2. \tag{2}$$

The objective is then to find the k sensing locations $(x_r(i), y_r(i))$. Hammel et al. [5] solved the above problem for the continuous measurements case (replacing the summations by integration). However, in our case since each measurement requires sampling in multiple directions and takes up to a minute, we cannot afford continuous measurements. To compute the k discrete locations we impose a grid

about the current position of the robot with size $n \times n$. The total number of candidate points for sensing locations are n^2. Hence, to compute the k sensing locations, we consider each of the $\binom{n^2}{k}$ combinations as a candidate trajectory and compute the FIM given by 2.

In general, computing the FIM requires knowing the true target location. However, since we do not know this, we use the estimate of the target location obtained after the initialization step. In addition, this strategy computes all sensing locations a priori. As a result, the performance of this (open-loop) strategy depends on the initialization error, as we observe in the simulation and experimental results in Section V.

C. Greedy

Instead of computing a fixed path for the k measurements, we can instead use a greedy strategy which picks the next measurement location based on the current estimate and uncertainty of the target. Given the current robot position and target position, Greedy looks at all neighboring locations of the robot. At every location, we simulate all candidate measurements (e.g. by uniformly picking s samples between 0 to 360°). Using the current estimate, we can compute the posterior covariance by simulating an EKF update using these candidate measurements. Thus, for every neighboring location, we will have s posterior covariances. Greedy then picks the candidate location where the maximum determinant of these s posteriors is minimum. This ensures best worst-case uncertainty for the target's position in a greedy fashion. Instead of the best worst-case uncertainty, we can choose other heuristics (such as average-case) for the greedy.

We can extend the Greedy strategy to "look-ahead" k measurements instead of just the immediate. This is explored in the Enumeration tree strategy described next.

D. Enumeration tree

In this approach, we extend the objective function of Greedy, to minimize the worst-case uncertainty obtained after k measurements. We use a min-max tree to achieve this objective. We can think of the min-max tree as a game played by the robot with an adversary. At every location, the adversary can choose a measurement which maximizes the uncertainty ("bearing nodes"). The robot always chooses an action which minimizes the uncertainty the adversary can pick at the new location ("action nodes"). Hence, this strategy ensures that after all the measurements, the worst-case uncertainty in the position of the target is minimized. The worst-case occurs when all the measurements are affected by maximum noise. In general, measurements contain less than maximum noise, and hence we do better than this worst-case scenario. Any other strategy which involves fixing all the sensing locations a priori cannot guarantee this.

Our strategy consists of two main steps: building the min-max tree, and executing the strategy, which we describe next.

Building the min-max tree: The min-max tree consists of two types of nodes: "bearing nodes" and "action nodes". Both type of nodes store the position of the robot and the uncertainty of the fish. The initial uncertainty along with the starting position of the robot is stored in the root node. We then assign the neighbors of the robot's current location as the children of the root node, and denote these as "action nodes".

To find the direction with maximum strength we sample every 15° from $0-180^\circ$ yielding 12 directions. Since we do not know the true location of the fish, we cannot determine which of these 12 corresponds to the actual measurement. Each of these 12 directions is a candidate for the true bearing measurement. Corresponding to each direction, we assign "bearing nodes" to each action node. The bearing nodes store the candidate bearing direction, in addition to the state of the robot and the uncertainty of the fish. We store the same position of the robot as that of its parent action node. We merge the uncertainty of the parent with the candidate bearing measurement using EKF updates, and store the resulting uncertainty.

For each bearing node, we again assign action nodes corresponding to each of the neighboring robot states on the grid. The uncertainty at each action node is the same as its parent bearing node. We can now recursively build the tree up to a depth $2k$ (so that there are k levels of bearing nodes).

Once the tree is built, the min-max value for each node is propagated in a bottom-up fashion starting with the leaf. The min-max value for the leaf nodes is defined as the determinant of the posterior covariance matrix stored at that node. If the min-max value for a node i is denoted using $M(i)$ we have the following recurrence,

$$M(i) = \begin{cases} |P_{i|i}|, & \text{if } i \text{ is a leaf node} \\ \max_{j \in C(i)} M(j), & \text{else if } i \text{ is } \textit{action node} \\ \min_{i \in C(i)} M(j), & \text{else if } i \text{ is } \textit{bearing node} \end{cases}$$

where $C(i)$ are the children of i^{th} node, and $P_{i|i}$ is the determinant of the posterior covariance after i measurements.

Executing the min-max tree: At the root node, we choose an action node with minimum min-max value. We take a new measurement after traveling to the location given by this action node. We now re-define the root of the tree to correspond to the bearing node corresponding to this measurement. Since we use discrete measurement samples while building the tree, we need to find that child node which is closest to the obtained measurement. We use the *Bhattacharya Distance* to find a child node, whose posterior covariance is closest to the current covariance (after the measurement update). The robot then repeats the above steps till it reaches the leaf nodes (corresponding to the k^{th} measurement location).

V. Experiments

To validate the proposed algorithms, we conducted both simulations and experiments using the system described in Section III.

A. Simulations

We first compared the three active localization strategies in simulation. We ran 100 random trials for each: the same

randomization seed was used across strategies. In each case, the robot started from the same initial position and the target was placed at the same location. We generated noisy bearing measurements by corrupting the true bearing with Gaussian noise (zero-mean and variance $\sigma_z = 15°$). The rest of the simulation parameters are listed in Table I.

The robot first executed the initialization step described in Section IV-A. Since the seed for randomization was the same, the resulting initial uncertainty was the same for corresponding trials for each strategy (but different across trials within the same strategy).

The results from the simulation are presented in Table II, and the corresponding histograms of final error and determinant of the final covariance matrix are shown in Figures 3 and 4 respectively. The outliers with large errors resulted from poor initial estimates. From the results we observe that Enumeration tree has lower mean final error and final uncertainty (determinant), where as the FIM strategy performs the worst of the three. This result is not surprising for two main reasons: (1) Since true target location is unknown, we compute the FIM using its initial estimate. Hence depending on how far the initial estimate is from the true, the measurement locations generated could be worse. (2) The FIM strategy computes locations which minimize the lower bound on the final uncertainty of an "efficient estimator" (i.e. estimator whose variance is equal to the CRLB). Since the EKF is not an efficient filter, there is no guarantee that it would achieve this lower bound. On the other hand, the Enumeration tree and the Greedy actually compute the covariance of this EKF estimator and pick the location which would minimize its determinant.

Hence, we decided to compare only the Enumeration tree and the Greedy strategy in actual experiments. The results from these experiments are presented next.

TABLE I

SIMULATION PARAMETERS

No. of trials	100	σ_z	$15°$
No. of measurements	3	r_{max}	$30m$
Step size	$3m$	Grid size	$60m \times 60m$

TABLE II

SIMULATION RESULTS FOR 100 TRIALS

Method	Mean final error	Mean final uncertainty
Enumeration tree	$5.7275m$	48.36
Greedy	$5.9809m$	40.59
FIM	$6.2975m$	54.81

B. Experiments on the robot

Experiments were conducted outdoors using the Husky robot and tracking equipment shown in Figure 1. The experimental setup is shown in Figure 5(a). A reference tag was kept at a location marked with a star, with its GPS coordinates noted for ground truth. We conducted three trials

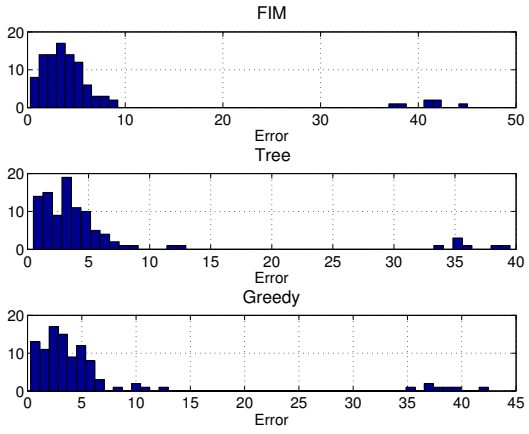

Fig. 3. Histogram of final error in simulation for all three strategies, for 100 trials with 3 measurements each. The mean errors for FIM, Enumeration tree and Greedy were $6.30m$, $5.73m$ and $5.98m$ respectively

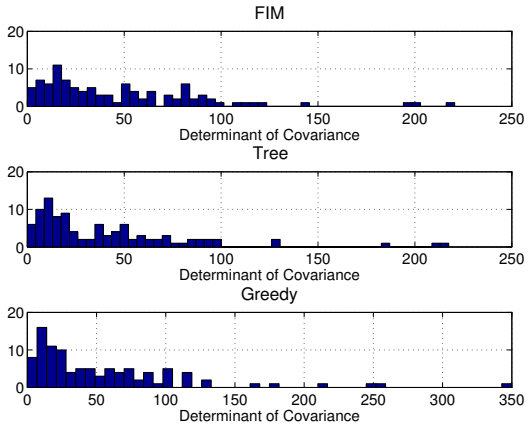

Fig. 4. Histogram of determinant of the final covariance matrix in simulation for all three strategies, for 100 trials with 3 measurements each. The mean values for FIM, Enumeration tree and Greedy were 48.36, 40.59 and 54.81 respectively

each using the Enumeration tree and the Greedy strategy to determine two measurement locations, in addition to those determined by executing the initialization method described in Section IV-A.

The results from one such trial with the Enumeration tree and Greedy are shown in Figures 5(b) and 5(c), respectively. The robot's mean estimated positions are labeled by green circles, while estimates of fish locations are shown as blue crosses. The true location of the tag is marked with a red star. The statistics from all experiments are presented in Table III.

Consider the trial shown in Figure 5(b). The first measurement was taken at the origin (R_1) by sampling the signal strengths in all directions, as described in Section III-C. The initial target bearing thus found was $38°$ from the X-axis. Using the initialization strategy, a second measurement location of $R_2 = (2, 10)$ was picked. The measured target bearing at this location was $-10°$. Using these two measurements, the initial estimate for the position of the target was found to be $(12.22, 9.07)$ with uncertainty $\sigma_x^2 = 33.36, \sigma_y^2 = 12.15$. The 1-$\sigma$ bound from this measurement is shown as the largest

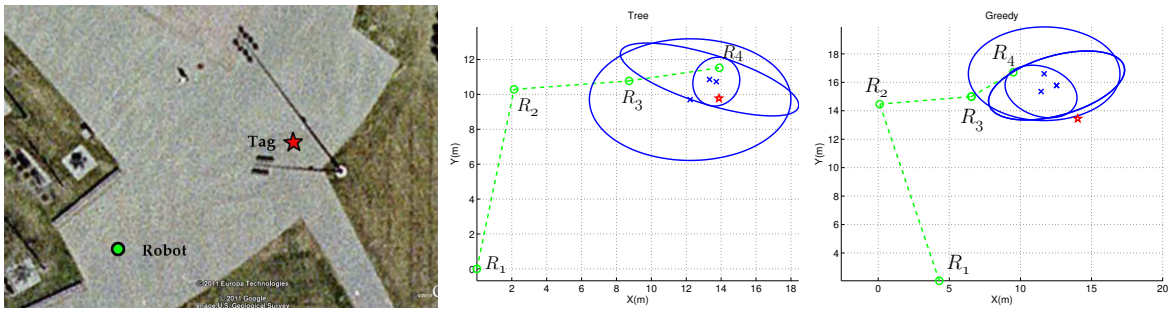

(a) Experimental setup. (b) Enumeration Tree Strategy (depth 2) (c) Greedy Strategy

Fig. 5. Setup and experimental results for two strategies. R_1 and R_2 are the two locations used for initialization. R_3 and R_4 are the measurement locations obtained using the corresponding strategy. The estimates at R_2, R_3 and R_4 are shown along with the corresponding 1-σ ellipse bounds. The true location of the tag is marked by a star.

blue ellipse.

The next two measurement locations (R_3, R_4) were calculated using the Enumeration Tree. From position $(10, 10)$ the robot measured the target bearing of 7° and at $(14, 13)$, this was 93°. Since the radio antenna has bimodal characteristics, a bearing of 93° also corresponds to a bearing of -87°. The final estimate of the target from the EKF was $(13.72, 10.73)$, which was within 2 meters of the true position. The final covariance from the EKF is shown in Figure 5(b) with the smallest blue ellipse.

TABLE III
EXPERIMENTAL RESULTS WITH DEPTH 2

Method	Final error	Final uncertainty
Enumeration Tree	0.97	3.53
	3.32	8.57
	5.35	6.04
Greedy	3.21	20.52
	3.29	11.93
	8.65	11.34

Figure 5(c) shows a similar trial with measurement locations computed using the Greedy strategy. The final estimate of the target for this trial was within 3.29 m of the true location. The results from other trials are given in Table III. The Enumeration tree strategy performs slightly better than Greedy, both in terms of final error and final uncertainty. However, the performance gains are a trade-off with respect to the significant computation time and space required for building the tree.

VI. CONCLUSION

We presented a novel system for localizing radio-tagged carp in frozen lakes. We studied the problem of choosing sensing locations in order to minimize the uncertainty in the target's location. We proposed three strategies, compared them in simulations and reported results from field experiments which show that our system is capable of localizing the target within a meter of the true location.

Since the fish move very little for long periods of time in winter, in our algorithms we assume that the target is stationary. When this assumption is violated, algorithms which address the mobility of the target must be designed. We are working on a complementary system that uses robotic boats as the underlying platform for tracking fish in the summer. In addition to the mobility of the fish, the motion of the boat during the measurement process makes the active localization problem harder. Our agenda for future research includes designing algorithms for this challenging problem.

VII. ACKNOWLEDGMENT

We thank the members of the Sorensen lab at the Department of Fisheries at the University of Minnesota for many useful discussions and sharing equipment. The Husky robot is provided by ClearPath Robotics through their PartnerBot program.

REFERENCES

[1] P. Bajer, G. Sullivan, and P. Sorensen, "Effects of a rapidly increasing population of common carp on vegetative cover and waterfowl in a recently restored Midwestern shallow lake," *Hydrobiologia*, vol. 632, no. 1, pp. 235–245, 2009.

[2] L. Nolfo and E. Hammond, "A novel method for capturing and implanting radiotransmitters in nutria," *Wildlife Society Bulletin*, vol. 34, no. 1, pp. 104–110, 2006.

[3] G. McMichael, M. Eppard, T. Carlson, J. Carter, B. Ebberts, R. Brown, M. Weiland, G. Ploskey, R. Harnish, and Z. Deng, "The juvenile salmon acoustic telemetry system: a new tool," *Fisheries*, vol. 35, no. 1, pp. 9–22, 2010.

[4] B. Johnson, T. McCoy, C. Kochanny, and R. Cook, "Evaluation of vaginal implant transmitters in elk (Cervus elaphus nelsoni)," *Journal of Zoo and Wildlife Medicine*, vol. 37, no. 3, pp. 301–305, 2006.

[5] S. E. Hammel, P. T. Liu, E. J. Hilliard, and K. F. Gong, "Optimal observer motion for localization with bearing measurements," *Computers and Mathematics with Applications*, vol. 18, no. 1-3, pp. 171 – 180, 1989.

[6] Y. Oshman and P. Davidson, "Optimization of observer trajectories for bearings-only target localization," *Aerospace and Electronic Systems, IEEE Transactions on*, vol. 35, no. 3, pp. 892 –902, July 1999.

[7] A. Bishop and P. Pathirana, "Optimal trajectories for homing navigation with bearing measurements," in *Proceedings of the 2008 International Federation of Automatic Control Congress*, 2008.

[8] A. Logothetis, A. Isaksson, and R. Evans, "An information theoretic approach to observer path design for bearings-only tracking," in *Decision and Control, 1997., Proceedings of the 36th IEEE Conference on*, vol. 4. IEEE, 1997, pp. 3132–3137.

[9] E. Frew, "Observer trajectory generation for target-motion estimation using monocular vision," Ph.D. dissertation, Stanford University, 2003.

[10] P. Skoglar, U. Orguner, and F. Gustafsson, "On information measures based on particle mixture for optimal bearings-only tracking," in *Aerospace conference, 2009 IEEE*. IEEE, 2009, pp. 1–14.